

PCCP

Accepted Manuscript



This is an *Accepted Manuscript*, which has been through the Royal Society of Chemistry peer review process and has been accepted for publication.

Accepted Manuscripts are published online shortly after acceptance, before technical editing, formatting and proof reading. Using this free service, authors can make their results available to the community, in citable form, before we publish the edited article. We will replace this *Accepted Manuscript* with the edited and formatted *Advance Article* as soon as it is available.

You can find more information about *Accepted Manuscripts* in the [Information for Authors](#).

Please note that technical editing may introduce minor changes to the text and/or graphics, which may alter content. The journal's standard [Terms & Conditions](#) and the [Ethical guidelines](#) still apply. In no event shall the Royal Society of Chemistry be held responsible for any errors or omissions in this *Accepted Manuscript* or any consequences arising from the use of any information it contains.

Cite this: DOI: 10.1039/c0xx00000x

www.rsc.org/xxxxxx

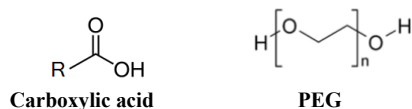
ARTICLE TYPE

Gaussian analysis of Raman spectroscopy of acetic acid reveals significant amount of monomers that effectively cooperate with hydrogen bonded linear chains

Jianping Wu^a

Received (in XXX, XXX) Xth XXXXXXXXX 20XX, Accepted Xth XXXXXXXXX 20XX
DOI: 10.1039/b000000x

Gaussian analysis of Raman spectroscopy reveals three significant structures in the liquid acetic acid (AA): linear chains involving C–H•••O=C and O–H•••O=C hydrogen bonding, cyclic dimers and dissociated monomers that can effectively cooperate with hydrogen bonded stacks of linear AA or polymer chains.



Scheme Molecular structure of carboxylic acid and PEG

The molecular structure of carboxylic acids (refer to Scheme) is of interest with respect of hydrogen bonding. They are simple model molecules in terms of studying interactions between carboxyl group and surrounding molecules and known to form the stable cyclic dimer that shows the strong double-bridged O–H•••O=C (dots) hydrogen bonding.¹ It was realized that AA, the simplest carboxylic acid, exists in a mixture of predominantly cyclic dimers and monomers in the vapour phase <math><150^{\circ}\text{C}</math> and linear chains that involve C–H•••O=C and O–H•••O=C hydrogen bonding in the solid crystalline form,³ respectively. Information on the liquid AA structure is, however, more limited than in the gas and solid state, which can be derived from electron and X-ray diffraction measurements respectively. A way to explore the liquid AA structure is to use vibrational molecular spectroscopy aided by theoretical simulations, which, however, led to two predominant but controversial liquid AA structures of either chains/clusters⁴ or dimers/short structures,⁵ with insufficient consideration of dissociated monomers⁶ for both. This is largely due to the difficulties of assigning a bond to specific hydrogen bonding when direct structural measurements are not available and also the greater diversity of hydrogen bonding in the liquid state,^{6b} particularly with respect of dissociated AA monomers.^{6a}

In principle, reduction of one hydrogen bonding structure within one liquid system would result in the increase of the others (one or more), or vice versa. Therefore, most interpretation of vibrational molecular spectroscopy of AA in the liquid state made before was disputable due to the lack of simultaneous consideration of the overall hydrogen bonding structures within each complete binary system of AA studied. In this report, liquid

AA structure was reinvestigated through Gaussian analysis of Raman spectroscopy obtained from 4 AA binary systems, namely, AA and EG ($n=1$), DEG ($n=2$), PEG300 or 400 (built up by repetition of the same simple unit) (refer to Scheme), respectively. The overall hydrogen bonding structures and their gradual changes within each four binary systems were considered together, respectively. In addition, Gaussian analysis was performed on Raman spectroscopy in the range corresponding to not only the O=C double bond but also the single bonds of AA that were scarcely studied before.

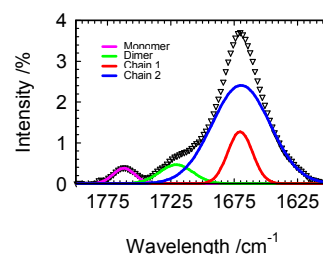
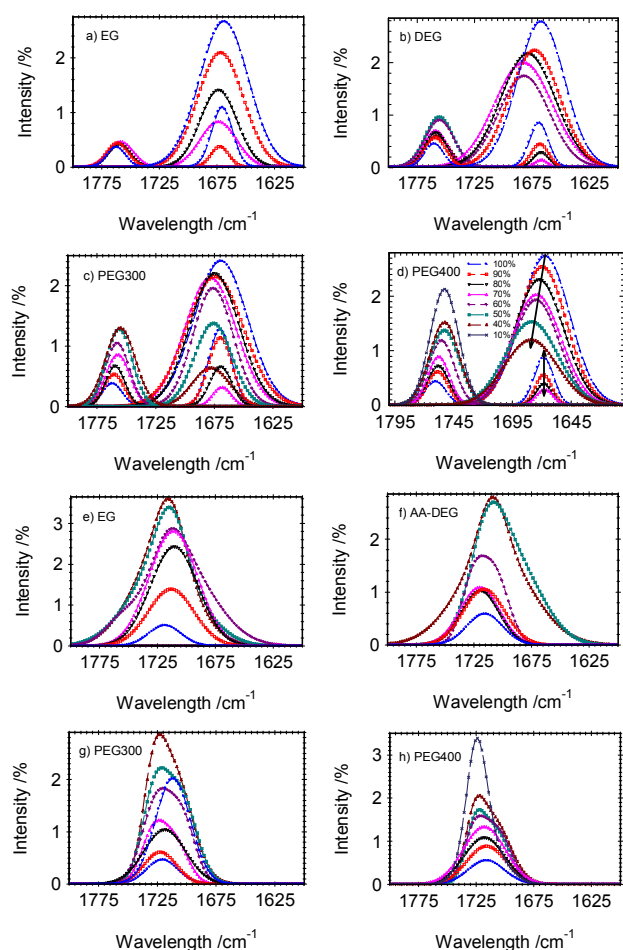


Fig. 1 Raman spectroscopy of O=C bond of AA (black open triangle) and Gaussian modes assigned to AA monomer (pink), cyclic dimer (green) and linear chains that involve C–H•••O=C (blue) and O–H•••O=C (red) hydrogen bonding.

The baseline corrected Raman spectroscopy of the O=C bond of AA (open triangle) and its de-convoluted 4 Gaussian modes^f (solid lines) are shown in Fig.1, in which there are no interfered Raman signals from 4 co-solvents. In this report, four Gaussian modes were assigned to 3 significant structures of AA in the liquid state that were identified separately before, i.e., monomers (pink), cyclic dimers (green) and linear chains involving C–H•••O=C (blue) and O–H•••O=C (red) hydrogen bonding, respectively. In previous studies, the weak peak at ca. 1760 cm^{-1} was generally assigned to the end of linear chains or monomers but merely based on assumption rather than investigational studies. The pronounced peak at ca. 1670 cm^{-1} was generally treated as a linear hydrogen bonded chain, which could not be discriminated into two hydrogen bonding structures by using ordinary data analysis approaches such as derivatives.⁷ The assignment of the peak at ca. 1720 cm^{-1} was diverse and even controversial, which was completely missing in the solid form and found to increase with temperature in the gaseous phase.^{4a,6c}



5 **Fig. 2** Gaussian modes versus the volume fraction of AA in the binary systems of AA and EG (a&e), DEG (b&f), PEG300 (c&g) or PEG400 (d&h) respectively. The same colour code for the curves with respect of volume fraction of AA (refer to the legend in d) was used for 4 binary systems throughout this report.

10 Three significant AA structures (as assigned with 4 Gaussian modes depicted in Fig. 1) all changed with the volume fraction of AA in 4 binary systems. For better view, the change of the Gaussian modes of AA is displayed separately as shown in Fig. 2 a) to d) (monomers and linear chains) and 2 e) to h) (dimers and
 15 short structures) respectively. The population of the linear hydrogen bonded AA chains at ca. 1670cm^{-1} in Fig. 2 a) to d) decreased monotonically with initial addition of the co-solvent in all 4 binary systems. The AA chains that involve $\text{O}-\text{H}\cdots\text{O}=\text{C}$ and $\text{C}-\text{H}\cdots\text{O}=\text{C}$ hydrogen bonding eventually became missing in the 4 binary systems when the volume fraction of AA decreased to either 80 (EG) and 60% (DEG, PEG300 and PEG400) for the former or 60 (EG), 50 (DEG), 30 (PEG300) and 30% (PEG400) (not shown) for the latter respectively. This strongly suggests that the cooperative hydrogen bonded stacks of linear AA chains^{4b,6a,6c}
 20 collapsed in the binary systems due to the increased interaction with each 4 polar co-solvents through uncooperative hydrogen bonding. The constant peak position of the $\text{O}-\text{H}\cdots\text{O}=\text{C}$ hydrogen bonding (e.g. as marked by a vertical line with two arrows in Fig. 2d) suggest that it is very stable in the liquid;^{4a, 6c} whilst the
 25 shifted peak position to the higher wavenumber of the $\text{C}-\text{H}\cdots\text{O}=\text{C}$ hydrogen bonding (e.g. as marked by a tilt line with an

arrow in Fig. 2d) suggest that the cooperative hydrogen bonded stacks of linear AA chains gradually became loose^{4b,6a,6c} with less cooperative effectiveness and eventually collapsed with further
 35 addition of each co-solvent. In addition, the $\text{O}-\text{H}\cdots\text{O}=\text{C}$ structures from the fallen apart AA chains predominately converted to the strong double bridged cyclic dimers at ca. 1720cm^{-1} that monotonically increased in all 4 binary systems as indicated by the increased single Gaussian mode from the
 40 original 100 (neat AA) (blue curve) to the volume fraction of AA at 70% (pink curve) in Fig. 2 e) to h). The $\text{C}-\text{H}\cdots\text{O}=\text{C}$ structures from the fallen apart AA chains alternatively resulted in the overall increases of complex dimers and short structures⁵ as illustrated by the increased contours involving multiple Gaussian
 45 modes (not shown) instead of the single cyclic dimer mode below the volume fraction of AA at about 60% (purple curve) in Fig. 2 e) to h). The population of dissociated AA monomers at ca. 1760cm^{-1} also increased initially from the original neat AA (100%) due to the fallen apart AA chains, which, however,
 50 displayed different manners in the 4 binary systems. For instance, it increased monotonically from the original neat AA (100%) to the volume fraction of AA at 40% and even further to the maximum at 10% (refer to the legend in Fig. 2d) when the AA chains became not present in the binary system of AA and
 55 PEG400. This illustrated that the collapsed cooperative hydrogen bonded stacks of linear AA chains were replaced by those of the stronger linear PEG400 chains, which eventually resulted in the increase of the dissociated AA monomers. On the other hand, it remained almost the same in the binary system of AA and EG
 60 from the original 100% to the volume fraction of AA at 60%, but became absent below 50% when the cooperative hydrogen bonded stacks of AA chains collapsed completely as shown in Fig. 2a. This demonstrated that the collapsed cooperative hydrogen bonded stacks of AA chains were irreplaceable in the
 65 binary system of AA and EG so that the significant increase of predominate dimers and short structures were observed instead (refer to Fig. 2e). The relatively higher population of the dissociated AA monomers in the binary system of AA and the co-solvent with longer molecules/association/chains (in the order
 70 from EG to DEG, PEG300 and PEG400 as seen in Fig. 2a to 2d) confirmed that the cooperative hydrogen bonded stacks of AA or polymer chains are essential on the existence of the dissociated AA monomers in the liquid state. Evidently, the peak (ca. 1770cm^{-1}) depicted in Fig. 1 should be assigned specifically to the
 75 dissociated AA monomers rather than the end of hydrogen bonded AA chains that were absolutely missing, e.g. at 10% of AA in the binary systems of AA and PEG400 as seen in Fig. 2d. In addition, it was found that, with the increased co-solvent in the binary systems, 1) FWHM of two Gaussian modes of AA linear
 80 chains gradually reduced from ca. 56 and 22cm^{-1} for $\text{C}-\text{H}\cdots\text{O}=\text{C}$ and $\text{O}-\text{H}\cdots\text{O}=\text{C}$, respectively, in all 4 binary systems; 2) FWHM of monomers (ca. 28cm^{-1}) kept almost the same in the binary system of AA and EG (or DEG) but gradually increased in the binary system of AA and PEG400 (or PEG300), respectively; 3)
 85 FWHM of cyclic dimers (ca. 38cm^{-1}) increased suddenly in the binary systems of AA and EG (or DEG) but increased gradually in the binary system of AA and PEG400 (or PEG300), respectively. The changes of FWHM for 4 Gaussian modes of AA also support the different hydrogen bonding structures in the

binary systems of AA and the shorter (EG or DEG) or longer (PEG400 or PEG300) surrounding co-solvent molecules.

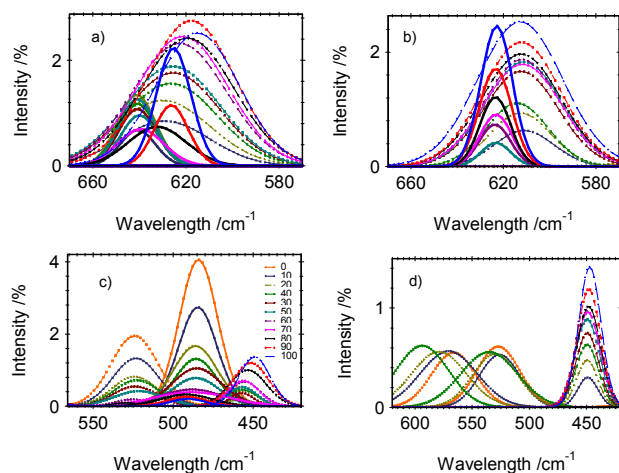


Fig. 3 Gaussian modes assigned to bend/deformation vibration of C-H bonds versus the volume fraction of AA in the binary systems of AA and EG (a) & (c) or PEG400 (b) & (d). The overlapped Raman Gaussian modes of AA and EG or PEG400 are displayed separately for better view.

The impact of hydrogen bonding on Raman spectroscopy should be perceptible in the range corresponding to the single bonds (C-C, C-O, C-H and O-H) as well as the mostly studied O=C double bond of AA, where in principle hydrogen bonding can form. It is anticipated that the impact of hydrogen bonding on the former is weaker and predominately interfered with that of the most organic solvents and, therefore, was scarcely studied before. Here, some preliminary results through Gaussian analysis with respect of bend/deformation vibration of C-H bonds from the binary systems of AA and EG or PEG400 are reported here respectively. As seen in Fig. 3 a) and c), the significant peak shift in three Gaussian modes of the C-H bond of AA (two in a) and one at ca. 450cm⁻¹ in c) are observed due to the collapsed cooperative hydrogen bonded stacks of AA chains irreplaceable by the shortest molecules/association of EG among 4 co-solvents studied; whilst the peak position of two Gaussian modes of EG itself at ca. 525 and 485cm⁻¹ in c) remain the same. Nevertheless, the same three Gaussian modes of AA (two in b) and one at 450cm⁻¹ in d) remain the same due to the collapsed cooperative hydrogen bonded stacks of linear AA chains replaced by those of stronger linear PEG400 chains; whilst the significant shift of the peak position of two Gaussian modes of PEG400 itself at ca. 575 and 525cm⁻¹ d) were observed respectively. The former could possibly suggest that AA changed from the cooperative hydrogen bonded stacks of AA chains^{4b,6a} to the disordered short AA aggregations,^{6b} whilst the latter illustrated that polymer PEG400 itself gradually changed from intramolecular to intermolecular hydrogen bonded chains through the interaction with the dissociated AA monomers and short structures. Similar changes of the Gaussian modes of AA and each four co-solvent molecules against the volume fraction of AA were also observed in Raman spectroscopy in the ranges corresponding to the other single bonds of AA, which will be reported in detail in future.

Conclusions

Through Gaussian analysis of Raman spectroscopy of the binary systems of AA and each four co-solvents sharing the same simple unit, the present study revealed the liquid structure of AA is somewhere in between the solid and gaseous state, in which the effective cooperativity of the overall hydrogen bonding structures takes the important role on stabilization of dissociated AA monomers.^{6b}

Notes and references

^a Pharmaterials, Ltd, A PII Company, 5 Boulton Road, Reading RG2 0NH, UK. Fax: +44 (0)1189310679; Tel: +44 (0)7738711594 E-mail: cheslhw@yahoo.co.uk

[†] Electronic Supplementary Information (ESI) available: details of preparation of the binary systems and measuring/processing Raman spectroscopy are available. See DOI: 10.1039/b000000x/.

- P. Waldstein and L. A. Blatz, *J. Phys. Chem.*, 1967, **71**, 2271; L. Turiand J. J. Dannenberg, *J. Phys. Chem.*, 1993, **97**, 12197-204; L. Turi, *J. Phys. Chem.*, 1996, **100**, 11285-91.
- M. D. Taylor, *Am. Chem. Soc.* 1980, **73**, 315; D. J. Frurip, L. A. Curtiss and L. A. Blander, *J. Am. Chem. Soc.*, 1980, **102**, 2610; J. Karle and L. O. Brockway, *J. Am. Chem. Soc.*, 1944, **66**, 574; J. L. Mol. Struct., 1971, **7**, 67.
- R. E. Jones and D. H. Templeton, *Acta Crystallogr.*, 1958, **11**, 484; I. Nahrungbauer, *Acta Chem. Scand.*, 1970, **24**, 453; P. G. Jonsson, *Crystallogr.*, 1971, **B27**, 893; R. Taylor and O. Kennard, *J. Am. Chem. Soc.*, 1982, **104**, 5063; G. R. Desiraju, *Acc. Chem. Res.*, 1991, **24**, 290.
- a) T. Nakabayashi, K. Kosugi and N. Nishi, *J. Phys. Chem. A*, 1999, **103**, 8595; K. Kosugi, T. Nakabayashi and N. Nishi, *Chem. Phys. Lett.*, 1998, **291**, 253; b) N. Nishi, T. Nakabayashi and K. Kosugi and *J. Phys. Chem. A*, 1999, **103**, 10851.
- O. F. aurskov Nielson and P. A. Lund, *J. Chem. Phys.*, 1983, **78**, 652.; P. Waldstein and L. A. Blaz, *J. Phys. Chem.*, 1967, **71**, 2271; I. A. Heisler, K. Mazur, S. Yamaguchi, K. Tominaga and S. R. Meech, *Phys. Chem. Chem. Phys.*, 2011, **13**, 15573; H. Pasalic, D. Tunega, A. J. A. Aquino, G. Haberhauer, M. H. Gerzabek and H. Lischka, *Phys. Chem. Chem. Phys.*, 2012, **14**, 4162; F. Genin, F. Quiles and A. Burneau, *Phys. Chem. Chem. Phys.*, 2001, **3**, 932.
- a) J. M. Briggs, T. B. Nguyen and W. L. Jorgensen, *J. Phys. Chem.*, 1991, **95**, 3315; W. Chen, C. Hsu and S. Lin, *Fluid Phase Equilibria*, 2013, **353**, 61; b) S. Imberti and D. T. Bowron, *J. Phys.: Condens. Matter*, 2010, **22**, 404212; J. Dong, Y. Ozaki and K. Nakashima, *Macromolecules*, 1997, **30**, 1111.
- J. P. Wu, M. J. Wang and J. W. P. Stark, *J. Quant. Spectrosc. Radiat. Transf.*, 2006, **54**, 773.